DOKUZ EYLÜL UNIVERSITY

GRADUATE SCHOOL OF NATURAL AND APPLIED SCIENCES

NUMERICAL INVESTIGATION OF MAGNETIC NANOFLUID BASED SINGLE PHASE NATURAL CIRCULATION LOOP

by

Selim Can BOZKIR

April, 2022

İZMİR

NUMERICAL INVESTIGATION OF MAGNETIC NANOFLUID BASED SINGLE PHASE NATURAL CIRCULATION LOOP

A Thesis Submitted to the
Graduate School of Natural and Applied Sciences of Dokuz Eylül University
In Partial Fulfillment of the Requirements for the Degree of Master of Science
in Mechanical Engineering, Energy Program

by

Selim Can BOZKIR

April, 2022

İZMİR

M.Sc THESIS EXAMINATION RESULT FORM

We have read the thesis entitled "**NUMERICAL INVESTIGATION OF MAGNETIC NANOFLUID BASED SINGLE PHASE NATURAL CIRCULATION LOOP**" completed by **SELİM CAN BOZKIR** under supervision of **ASSOC. PROF. DR. ALPASLAN TURGUT** and we certify that in our opinion it is fully adequate, in scope and in quality, as a thesis for the degree of Master of Science.

…………………………………………

Assoc. Prof. Dr. Alpaslan TURGUT

Supervisor

………………………………

Assoc. Prof. Dr. Mehmet Akif EZAN

(Jury Member)

…………………………………

Assist. Prof. Dr. Serkan DOĞANAY

(Jury Member)

Prof. Dr. Okan FISTIKOĞLU

Director

Graduate School of Natural and Applied Sciences

ACKNOWLEDGEMENT

First of all, I would like to sincerely thank my esteemed supervisor, Assoc. Prof. Dr. Alpaslan TURGUT, for his support he has given me in this thesis and my progress on the academic path and especially for the different perspectives he has given me. It was a great pleasure and honour for me to work with him.

Secondly, I am also grateful Assoc. Prof. Dr. Ziya Haktan KARADENIZ, Assist. Prof. Dr. Serkan DOGANAY and M.Sc. Nur COBANOGLU for their valuable support in my thesis and other works.

Finally and most importantly, I would like to thank my mother and father with all my heart for their efforts and support since my childhood. They have showed me the brightest way on the path I am on. I am so grateful for everything they have done for me. It is hard to find words to express my gratitude.

Selim Can BOZKIR

NUMERICAL INVESTIGATION OF MAGNETIC NANOFLUID BASED SINGLE PHASE NATURAL CIRCULATION LOOP

ABSTRACT

Single-Phase Natural Circulation Loop (SPNCL) systems are widely used passive heat transfer systems, and the density gradient caused by temperature difference and resulting buoyancy forces are the driving heat transfer mechanism. In this study, it is aimed to propose a Single-Phase Natural Circulation mini Loop (SPNCmL) under the influence of external magnetic field. This system works with a temperature sensitive ferrofluid under an external magnetic field which manipulates the ferrofluid flow propagation and temperature distribution by mangetic volume force and heat source effects. Within this scope, a numerical model is developed in COMSOL Multiphysics by coupling magnetic field (no currents), heat transfer in fluids and laminar flow modules. A NdFeB permanent magnet with a remanence of 1.22 T is located at the outlet of the cooler-end since the higher magnetization is obtained at lower temperatures. SPNCmL system is working with DIW-based Fe_3O_4 ferrofluids' (1-3 vol%.) concentration under the conditions of different heater powers (30 and 50 W). Applying an external magnetic field dramatically affects the system performance in terms of increase in ΔT_{heater} and ε up to 34% and 25% compared to water. Higher T_{max} values (up to 9%) are obtained for Fe_3O_4 ferrofluids compared to water, in contrast applying magnetic field results in an increment up to 5%. Additionally, the effect of magnetic field on the temperature distribution and flow propagation are evaluated by dimensionless temperature and velocity distributions at critical cross-sections of the cooler-end for better understanding.

Keywords: Ferrofluid, mini loop, natural convection, single phase, magnetic field, effectiveness.

MANYETİK NANOAKIŞKAN BAZLI TEK FAZLI DOĞAL TAŞINIM DÖNGÜSÜNÜN SAYISAL İNCELENMESİ

ÖZ

Tek Fazlı Doğal Taşınım Döngü sistemleri, yaygın olarak kullanılan pasif ısı transfer sistemleridir ve sıcaklık farkının neden olduğu yoğunluk gradyanı ve ortaya çıkan kaldırma kuvvetleri, itici ısı transfer mekanizmalarıdır. Bu çalışmada, harici manyetik alan altında Tek Fazlı mini Doğal Taşınım Döngüsünün incelenmesi amaçlanmıştır. Bu sistem, ferroakışkanın akış ve sıcaklık dağılımını manipüle eden harici bir manyetik alan altında sıcaklığa duyarlı bir ferroakışkan ile çalışır. Bu kapsamda COMSOL Multiphysics'te akımsız manyetik alan, akışkanlarda ısı transferi ve laminer akış birleştirilerek sayısal bir model geliştirilmiştir. Daha yüksek mıknatıslanma daha düşük sıcaklıklarda elde edildiğinden, soğutucu ucun çıkışına 1.22 T'lik bir kalıcılığa sahip bir NdFeB kalıcı mıknatıs yerleştirilmiştir. Tek Fazlı mini Doğal Taşınım Döngü sistemi, farklı ısıtıcı güçleri (30 ve 50 W) koşullarında deiyonize su bazlı Fe_3O_4 ferroakışkanların farklı (%1-3 hacim) konsantrasyonu ile çalışmaktadır. Harici bir manyetik alan uygulamak, ΔT_{heater} ve ε'de suya kıyasla %34 ve %25'e varan artış açısından sistem performansını önemli ölçüde etkiler. Suya kıyasla Fe_3O_4 ferroakışkanlar için daha yüksek T_{max} değerleri (%9'a kadar) elde edilir, aksine manyetik alan uygulanması %5'e varan bir artışla sonuçlanır. Ek olarak, daha iyi anlaşılması için, manyetik alanın sıcaklık dağılımı ve akış yayılımı üzerindeki etkisi, soğutucu ucun kritik kesitlerinde boyutsuz sıcaklık ve hız dağılımları ile değerlendirildi.

Anahtar kelimeler: Ferroakışkan, mini döngü, doğal taşınım, tek faz, manyetik alan, etkinlik.

CONTENTS

Page

LIST OF FIGURES

LIST OF TABLES

CHAPTER ONE
INTRODUCTION

Single-Phase Natural Circulation Loops (SPNCLs) are heat transfer systems whose driving mechanism is the buoyancy forces as a result of density gradient caused by temperature difference. Considering their superiorities of simplicity, maintenance free, improved safety, investigations on the achieve high performance SPNCL have been increasing. Geometrical parameters (pipe diameter, shape, size, aspect ratio and heater-cooler orientation), condition of operation and the working fluid’s properties have a strong effect on the SPNCL performance (Çobanoğlu et al., 2019).

Nanofluids are suspension of nanosized particles in base fluids (Choi & Eastman, 1995). Within the scope of working fluids, nanofluids as suspension of nanosized particles in conventional heat transfer fluids, (as a base fluid water (DIW), oil, ethylene glycol, oil, etc. can be used.) are considered as a new type of heat transfer fluids since they have the ability of improving heat transfer performance a result of higher thermal conductivity with a penalty of higher viscosity (Choi & Eastman, 1995). Although nanofluids have been widely used in applications of forced convection, their superiority in passive heat transfer systems is getting attention (Cobanoglu & Karadeniz, 2020). In SPNCLs, utilization of nanofluids end up improved heat transfer performance, improved stability and decrement in the required time for steady operation.

The demand on the miniaturization of the high technology devices requires further investigations on the dissipation of higher heat rates from the core components of these devices. Within this scope, SPNCLs are miniaturized to be applicable in small-scale applications such as micro-electronics (Çobanoğlu et al., 2019) (Garibaldi & Misale, 2008). Miniaturization of a SPNCL is the reduction of its dimensions to tens of centimeters and diameters of pipes to a few millimeters and does not affect the driving mechanism of the loop (Cobanoglu & Karadeniz, 2020). Improvement in stability can also be obtained by the Single-Phase Natural Circulation mini Loops (SPNCmLs) (Misale et al., 2007). Misale et al. (Misale et al., 2007) investigated first SPNCmL system. They utilized different operational conditions, such as, different inclination angles (0, 30, and 75˚), heater power (2.5 – 25 W). They observed that the best thermal performance at 0˚ inclination angle and 25 W power by comparing difference of temperature between heater and cooler outlet. Nayak et al. (Nayak et al., 2008) studied experimentally, first SPNCL system with nanofluid. They utilized alumina-water nanofluid with different concentrations (0.3-2 % by weight 40 – 80 nm particle size). They observed that using nanofluids provides an operation at elevated power level than usual. Misale et al. (Misale et al., 2012) investigated the performance of nanofluid-based SPNCmL, for the first time. Utilization of the nanofluids resulted in a slight enhancement in the thermohydraulic performance of the SPNCmL compared to DIW for only inclined loop orientations, but in general, the performance of the nanofluids is comparable with the DIW. However, Turgut and Doğanay (Turgut & Doganay, 2014) reported that higher nanofluid concentrations caused higher effectiveness which is used for the SPNCmL's thermal performance's evaluation for the first time in this study. Karadeniz et al. (Karadeniz et al., 2014) created a numerical model based on the experimental study of Turgut and Doğanay (Turgut & Doganay, 2014). The proposed numerical model has the potential to conduct comparative parametric analyses to predict the performance and characteristics of SPNCmLs within an error band of ± 10%. Ho et al. (Ho et al., 2014) worked about nanofluid based SPNCmL with mini channel heat sink and heat source. They investigated effect of the nanofluid's weight concentration and wall temperature difference between natural circulation loop's hot and cold ends. As a nanofluid they utilized alumina-water. As a result of their study, they observed that alumina-water nanofluid can enchanced the natural circulation loop's heat transfer performance. Doğanay and Turgut (Doganay & Turgut, 2015) investigated the effect of inclination angles and heat sink temperatures on the performance of SPNCmL operating with DIW based Al_2O_3 nanofluid. They concluded that lower heat sink temperatures and greater inclination angles result in higher effectiveness values. Karadeniz et al. (Karadeniz et al., 2016) improved the previously proposed numerical model by investigating the inclination angle effect on the SPNCmL performance. The proposed steady model in analyzes match up with data of experiment at low heater power and low volumetric concentrations and the deviation increased up to 10% with increasing heater power and concentrations. Koca et al.

(Koca et al., 2017) found that effectiveness did not change with the heater power for SPNCmL working with higher concentrations of the DIW based Ag nanofluid. However, smaller concentrations have higher effectiveness at higher heater powers and similar thermal stability with SPNCmL working with DIW. Different from water-based nanofluids, Mohan et al. (Mohan et al., 2014) investigated hexagonal boron nitride and mineral-oil based nanofluid's efficiency in SPNCmL with the orientation of horizontal heater horizontal cooler. When compared with water, they observed the temperature difference was increased between 2% and 7.4% as increasing of power.

Ferrofluids, as another kind of nanofluids, are suspensions of ferromagnetic nanoparticles (iron, cobalt, nickel, magnetite, hematite, etc.) dispersed in non-magnetic basefluids (Buschmann, 2020). In 1963, Steve Papell invented ferrofluids for making a suitbale liquid rocket fuel which which could be attracted by an external magnetic field towards the pump's inlet in a zero-gravity environment (Kole & Khandekar, 2021). Ferrofluids have application potential in many fields such as energy harvesters, solar systems, nuclear systems, heat transfer, etc. (Doganay et al., 2019). Among them, heat transfer applications have attracted researchers' interest, due to the tunable thermophysical properties, and the manipulation capability of the ferromagnetic nanoparticles under the influence of the external magnetic field (Doganay et al., 2019).

The ferrofluid-based loops are originated in 1977 and introduced as an automatic cooling device (Matsuki et al., 1977). They used water-based Mn-ferrite nanofluid in the proposed cooling device. The SPNCL has a vertical heater and vertical cooler configuration, and the electromagnets are located at the inlet of the heating end. It was mentioned that this ferrofluid-based cooling device has two superiorities which are automatic control by the thermal state of the device to be cooled and the no need for a pump for fluid flow. Utilization of the permanent magnets in addition to the heat source and heat sink was reported to be the driving mechanism of the fluid flow. Investigations on the ferrofluid-based automatic energy transport device (AETD) have been increasing during the last decade. Thermomagnetic effect can be explained as a when the external magnetic field utilized to magnetic fluid, the hotter fluid is less magnetised than a cooler fluid (Fruh, 2005). And thus, it creates gradient with the effect of this magnetization differences. In these thermomagnetic loop systems, by generating a magnetic force on the ferrofluid, the magnets are also responsible for the fluid flow together with heat sinks and heat source and these combinations are called as “pumps” (Lian et al., 2009). Lian et al. (Lian et al., 2009) have shown that the energy transport process could be controlled by an external magnetic field and/or temperature changes of the ferrofluid in miniature AETD, and the fluid velocity increased with increasing heater power. They have experimentally investigated three different types of the AETD: single magnet pump square loop, two magnets pump loop and the toroidal loop. The square loops have a horizontal heater and a vertical cooler orientation. Two magnets pump loop had the best performance among all. Lian et al. (Lian et al., 2010) proposed a theoretical study and developed a numerical model to investigate thermomagnetic convection loop systems by increasing the number of magnets. The connection type and the number of the “pumps” affect the fluid flow and heat transfer characteristics strongly. Xuan and Lian (Xuan & Lian, 2011), investigated two different configurations of the magnet in the loop system and the effect of the blower to imply AETD in electronic chip cooling applications. Locating the magnet closer to the heat source had better cooling performance and a steadier start-up. In the toroidal loop system of Chaudhary et al. (Chaudhary et al., 2017), increase of the heat load results in a reduction in the magnetization of the water-based Mn-Zn ferrite ferrofluid and higher fluid velocity, thus faster heat transfer between the heat sink and heat source. They also developed a numerical model based on their experimental setup and reported a good agreement with the experimental data. Aursand et al. (Aursand et al., 2016) have investigated the effects of kerosene based Mn-Zn ferrite nanofluid on natural convection cooling loop under constant temperature boundary conditions. They have found that effect of thermomagnetic driving force is notable compared to natural convection and results in at least 50% cooling performance enhancement. Moreover, thermomagnetic force enabled the more compact solutions such as elimation of rig height and heat sink with 25% smaller size while retaining original performance. Karimi-Moghaddam et al. (Karimi-Moghaddam et al., 2014) developed a 1D theoretical model to characterize thermomagnetic circulation in the loop under laminar flow conditions and 3D numerical model in COMSOL Multiphysics to use results in 1D model. Geometric length scales, magnetic fluid properties and strength of the employed magnetic field were investigated parameters in the theoretical model. They achieved a higher velocity gradient near the heat source resulting increment of heat transfer in this section compared to cooler section. Moreover, they developed a Reynolds number correlation as a Grashof number's function and geometrical parameters, and Nusselt number correlation as a function of Rayleigh number. Moreover, they mentioned that Curie temperature, the temperature at net magnetization is zero (Love et al., 2005), and the magnetic field strength are the most important parameters affecting device performance (Karimi-Moghaddam et al., 2013). Placing magnets near the heater inlet results in attraction of the magnetic fluid towards regions with higher field strength and in this region difference between fluid temperature and Curie temperature is getting smaller. Smaller temperature difference results in losing attraction of the fluid to magnetic field and it displaced by colder fluid. Temperature gradient at the fluid cross-section causes different magnetic properties of the ferrofluid. Weak magnetization due to the smaller temperature difference results in higher velocities near the tube walls and fluid have lower velocity at the central region. Phor and Kumar (Phor & Kumar, 2019) located the magnet near the heat source inlet of the loop system having vertical heater vertical cooler orientation. Higher loads of heat source resulted in larger driving force and thus enhanced cooling. Moreover, the working fluid's concentration increase (3 to 7 vol.%) improved the cooling performance by 11%. Utilization of the 0.3 T magnet in the system enhanced the device performance by 8%.

As mentioned above, thermomagnetic convection is the main heat transfer mechanism in the AETDs and its effect on the device performance is generally investigated by placing magnets near the heater inlet. Considering the strengthen magnetization by increasing the difference between fluid temperature and Curie temperature for better heat transfer performance, this thesis aims to investigate the effects of placing magnets near the cooler-end outlet on the SPNCmL performance and the natural convection dominancy considering the fluid flow and the temperature distributions, numerically. The numerical model is developed in COMSOL Multiphysics by coupling magnetic field (no currents), heat transfer in fluids and fluid flow (laminar flow). SPNCmL working with water based Fe_3O_4 ferrofluid has the horizontal heater and horizontal cooler configuration. Since the higher magnetization is obtained at lower temperatures, the 1.22 T NdFeB magnet is located at the cooler outlet. Table 1.1 provides a brief summary of different works performed by other authors.

Table 1.1 Some available studies in literature.

Authors	Investigations	Findings
(Misale et al., 2007)	Different inclination angles, heater power are investigated. First SPNCmL system.	The best thermal performance at 0˚ inclination angle and 25 W power.
(Nayak et al., 2008)	Different concentrations. First SPNCL system with nanofluid.	Using nanofluids provides an operation at elevated power level than usual.
(Misale et al., 2012)	Different inclination angles, heater power, heat sink temperature are investigated.	Utilization of the nanofluids resulted in a slight enhancement in the thermohydraulic performance of the SPNCmL compared to DIW for only inclined loop orientations.
(Turgut & Doganay, 2014)	Different particle size and concentrations of nanofluids are investigated.	Higher nanofluid concentrations caused higher effectiveness which is used for the evaluation of SPNCmL’s thermal performance for the first time. Thermal performance enhancement of the system is more remarkable with bigger particle size.
(Ho et al., 2014)	Different nanofluid concentrations are investigated.	Alumina-water nanofluid can enchanced the natural circulation loop’s heat transfer performance.

Table 1.1 Continues

(Doganay & Turgut, 2015)	Effect of inclination angles and heat sink temperatures on the performance of SPNCmL investigated.	Lower heat sink temperatures and greater inclination angles result in higher effectiveness values.
(Koca et al., 2017)	Different concentrations and heater powers are investigated.	Effectiveness did not change with the heater power for SPNCmL working with higher concentrations of the DIW based Ag nanofluid.
(Matsuki et al., 1977)	Water-based Mn-ferrite nanofluid is used in the proposed cooling device.	This cooling device has two superiorities which are automatic control by the thermal state of the device to be cooled and the no need for a pump for fluid flow.
(Lian et al., 2009)	Investigated three different types of the automatic energy transport devices (AETD).	Two magnets pump loop had the best performance.
(Lian et al., 2010)	Different number of magnets are utilized.	The connection type and the number of the “pumps” affect the fluid flow and heat transfer characteristics strongly.
(Chaudhary et al., 2017)	Different nanofluid concentrations are investigated. For the first time, the switching (application and removal of magnetic field between measurements) effect of magnetic field on cooling was studied.	Heat load increases, the magnetization of the ferrofluid decreases; leading to an increase in the fluid velocity and consequently, faster heat transfer from the heat source to the heat sink.

Table 1.1 Continues

(Aursand et al., 2016)	Effect of kerosene based Mn-Zn ferrite nanofluid is investigated on natural convection cooling loop.	Effect of thermomagnetic driving force is notable compared to natural convection and results in at least 50% cooling performance enhancement.

CHAPTER TWO
MATERIALS AND METHODS

2.1 Numerical Model

The developed model in analyzes was created by coupling of three different physics in COMSOL Multiphysics. In multiphysics interface, magnetic field (no currents), heat transfer in fluids, and laminar flow physics were utilized. First, the magnetic field (no current) physic was utilized to the model by the effect of permanent magnet. In this physic; for magnet, 1.22 T remanent flux density is defined. For ferrofluid and air environment, relative permeability is defined as material dependent. Also, zero magnetic scalar potential boundary condition defined to the air environment. Following, the magnetic field effect on fluid flow and heat transfer added to the momentum and energy equations as the magnetic volume force (Sheikholeslami & Ganji, 2014; Tzirtzilakis & Xenos, 2013), and magnetocaloric effect terms (Sheikholeslami & Ganji, 2014; Tzirtzilakis & Xenos, 2013), respectively.

The permanent magnet generated magnetic field intensity in the SPNCmL region. The magnetic field intensity is determined by Gauss' Law for magnetism:

$$\nabla \cdot (\mu_0 \mu_r \mathbf{H} + \mathbf{B_r}) = 0 \tag{2.1}$$

where μ_0 is the free space permeability, μ_r and $\mathbf{B_r}$ are the relative permeability and remanence of the permanent magnet, respectively. Eq. 2.2 is solved for magnetic field intensity ($\mathbf{H}$) depending on the magnetic scalar potential (V_m) given as:

$$\mathbf{H} = -\nabla V_m \tag{2.2}$$

If the particles are superparamagnetic and well-suspended in the basefluid, the entire ferrofluid domain can be considered a homogenous medium (Gijs et al., 2010; Nguyen, 2012). Within the scope of this consideration, ferrofluid were modeled as a single phase domain. For a single phase ferrofluid medium, once the magnetic field intensity is obtained, the corresponding magnetic force ($\mathbf{F_m}$) and magnetocaloric effect ($\mathbf{Q_m}$) on the ferrofluid can be calculated as follows (Sheikholeslami & Ganji, 2014; Tzirtzilakis & Xenos, 2013):

$$\mathbf{F_m} = \mu_0 M \left(\frac{d\mathbf{H}}{dx} + \frac{d\mathbf{H}}{dy} + \frac{d\mathbf{H}}{dz}\right) \quad \left[\frac{N}{m^3}\right] \tag{2.3}$$

$$\mathbf{Q_m} = -\mu_0 T \,\frac{dM}{dT}\left(u\frac{d\mathbf{H}}{dx} + v\frac{d\mathbf{H}}{dy} + w\frac{d\mathbf{H}}{dz}\right) \quad \left[\frac{W}{m^3}\right] \tag{2.4}$$

Figure 2.1 shows that the magnitude of magnetic volume forces through the x direction of the cooler. It shows that, when the heater power and volumetric concentration are decreased, magnetic volume forces increase. Because, magnetization increases when the temperature decreases.

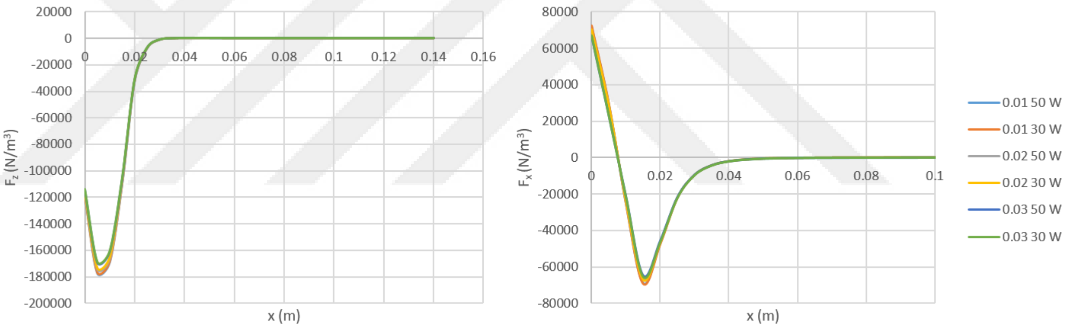

Figure 2.1 Magnetic volume forces (F_z and F_x) through the x direction of the cooler.

In Eq. 2.3 and 2.4, T is the temperature, u, v, w are the velocities in x, y, and z directions, respectively. M is the magnetization of the ferrofluid and it can be expressed by (Andersson & Valnes, 1998),

$$M = K(T_{curie} - T) \tag{2.5}$$

where K is the pyromagnetic coefficient (Bouhrour & Kalache, 2017) and T_{curie} is the Curie temperature. The magnitude of applied H is enough for the saturation as can be seen from the Figure 2.2b when compared with values at Figure 2.2a (Alsangur et al., 2021), thus, *M* can be assumed as linear equation (Andersson & Valnes, 1998). In Figure 2.2a, MF1 means Fe_3O_4, MF2 means γ-Fe_2O_3.

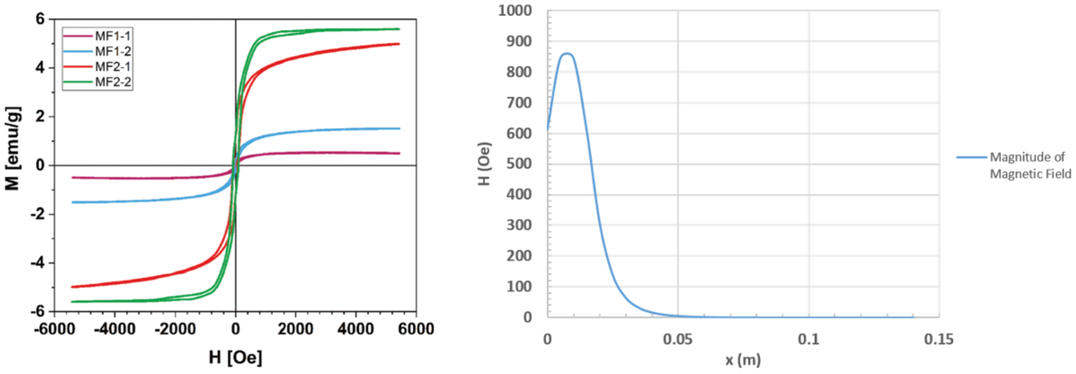

(a) (b)

Figure 2.2 a) H-M curves of ferrofluids (Alsangur et al., 2021) b) Magnitude of magnetic field in the cooler

Under the influence of the magnetic field, the steady state 3-D incompressible flow's governing equations' general form can be described as (viscous dissipation is neglected) (Sheikholeslami & Ganji, 2014; Tzirtzilakis & Xenos, 2013):

Continuity equation:

$$\nabla \cdot \mathbf{u} = 0 \tag{2.6}$$

Momentum equation:

$$\rho(\mathbf{u} \cdot \nabla)\mathbf{u} \;= -\nabla p + \nabla \cdot [\, \mu(\nabla \mathbf{u} + \nabla \mathbf{u}^{\mathrm{T}})\,] + \mathbf{F_{ext}} \tag{2.7}$$

Energy equation:

$$\rho C_p(\mathbf{u} \cdot \nabla T) \; + (\nabla \cdot q) = \mathbf{Q_p} + \mathbf{Q_m} \tag{2.8}$$

In the governing equations, **u** is the velocity vector [m/s], $\mathbf{F_{ext}}$ is external forces [N/m^3], $\mathbf{Q_p}$ is pressure work, and $\mathbf{Q_m}$ is heat source term due to the magnetocaloric effect [W/m^3] in Eq. 2.4. ρ, μ and C_p are density, viscosity, specific heat of the working fluid, respectively. External force (**F_{ext}=F_m+F_b**) in Eq. 2.7 includes a magnetic force term given in Eq. 2.3 and buoyancy term as follows

$$\mathbf{F_b} = (\rho - \rho_{ref})\mathbf{g} \tag{2.9}$$

In Eq. 2.9, ρ_{ref} is fluid's reference density, which is computed from the mean temperature of the fluid.

Figure 2.3 presents the schematic of the geometry and dimensions of the SPNCmL based on the experimental setup (Doganay & Turgut, 2015; Turgut & Doganay, 2014). In the heater part in this numerical study, heat flux defined as constant (30 and 50 W of heat rates for the surface area of the heater) and applied as the power input of heater, whereas in the cooler part, temperature defined as constant (T_C) and described as 293.15 K, which is the temperature of cooling fluid. Other parts of the system are thermally insulated and modeled as adiabatic. A NdFeB permanent magnet with a remanence of 1.22 T is located at the outlet of the cooler part with a vertical distance of 5 mm since the higher magnetization is obtained at lower temperatures (Phor & Kumar, 2019). The validation and mesh independency analysis of the numerical model are conducted for all three heater powers (10, 30 and 50W) used in the experimental study, and the results of validation study have been presented at Section 3.1. Mesh independency analysis was conducted for four different mesh element numbers (M1=203803, M2=937369, M3=1620296 and M4= 2603801). 10^{-7} was set to criteria of convergence. To evaluate the mesh independency T_{max} and ΔT_{heater} parameters, which are two ciritical parameters for the comparison of experimental and numerical data, were calculated with M1, M2, M3 and M4 at different heater power values. Figure 2.4 showed that using M3 is suitable for obtaining accurate solution and avoiding from waste of time.

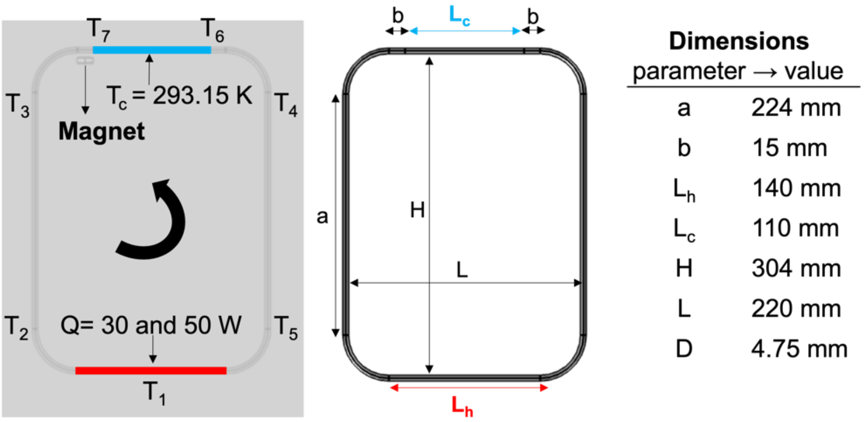

Dimensions

parameter → value	
a	224 mm
b	15 mm
L_h	140 mm
L_c	110 mm
H	304 mm
L	220 mm
D	4.75 mm

(a) (b) (c)

Figure 2.3 a) Schematic of the SPNCmL including positions of magnet and temperature probes, b) Geometrical parameters of SPNCmL, c) Dimensions of the SPNCmL corresponding to the given geometrical parameters.

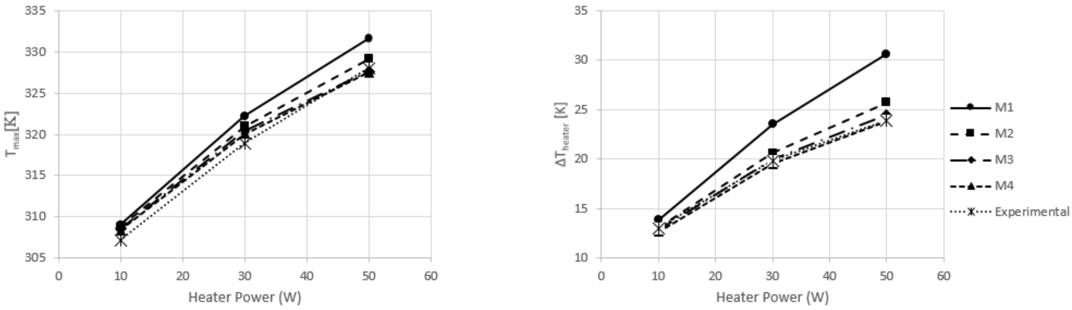

Figure 2.4 Mesh independency analysis.

2.2 Thermophysical Properties

For this thesis, fluids’ thermophysical properties are fitted to the numerical model as a function of temperature since the temperature-dependent thermophysical properties are important for the accurate prediction of the heat transfer performance of the SPNCmL (Cobanoglu & Karadeniz, 2020; Sahu et al., 2021). Temperature dependency of DIW’s thermophysical properties is provided by tabular values (Çengel & Cimbala, 2006). The existing models in the literature were utilized to predict effective specific heat (Zhou & Ni, 2008), density (Yu et al., 2008), and thermal expansion coefficient (Bourantas et al., 2014) of ferrofluid samples which are expressed by Eq. 2.10-2.12, respectively. DIW's temperature dependent properties are assumed as dominant parameters in the second-order polynomials as a function of temperature for each corresponding equation, and thermophysical properties of nanoparticles are kept constant. Thermophysical properties ($C_{p,p}$, ρ_p, β_p) of the nanoparticles are presented in the Table 2.1. The change of thermophysical properties with concentration at different temperatures is presented in Figure 2.5. Different concentration of ferrofluids (FF) are labeled as FF1, FF2 and FF3 for 1, 2 and 3 vol.%, respectively.

$$C_p = \frac{\sigma\left(C_{p,p}\rho_p\right) + (1-\sigma)(\rho_f(T)C_{p,f}(T))}{\sigma\rho_p + (1-\sigma)\rho_f} \tag{2.10}$$

$$\rho = (1-\sigma)\rho_f + \sigma\rho_p \tag{2.11}$$

$$\beta = \frac{\sigma\left(\beta_p\rho_p\right) + (1-\sigma)(\rho_f(T)\beta_f(T))}{\rho} \tag{2.12}$$

Here, σ is volumetric concentration of ferrofluid and T is the temperature [K].

Table 2.1 Density (T. M. Group) , specific heat (Grosu et al., 2017) and thermal expansion coefficient (Holcomb, 2019) of Fe_3O_4 nanoparticles.

	Density **ρ [kg/ m³]**	**Specific Heat** C_p **[J/kg K]**	**Thermal Expansion** β **[1/K]**
Fe_3O_4	5170	665.15	7.62×10^{-6}

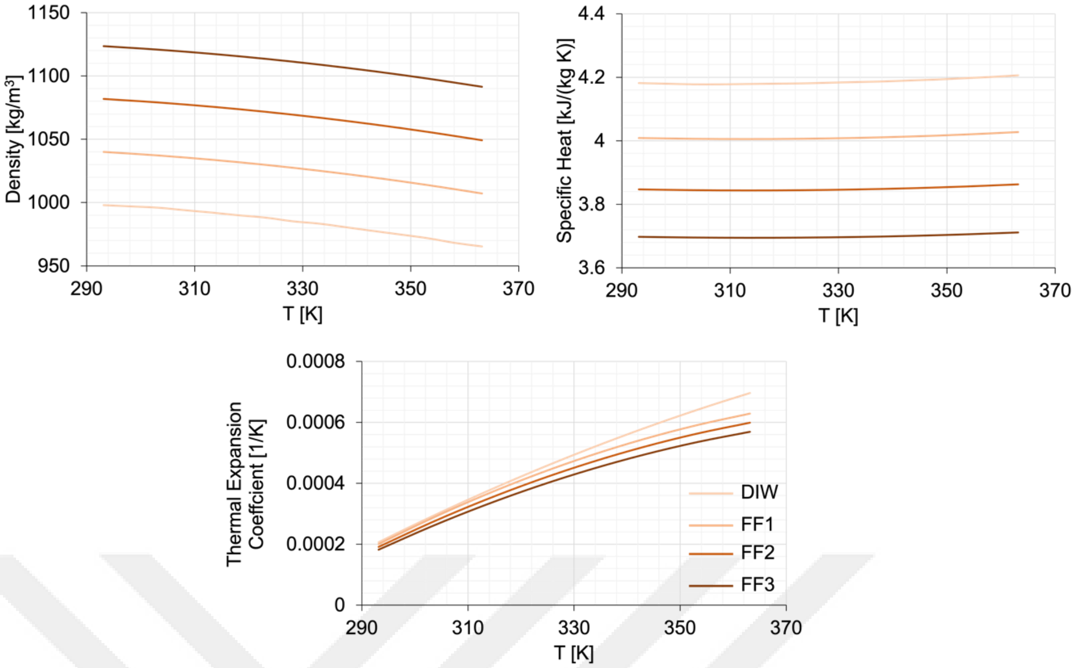

Figure 2.5 The variation of effective specific heat, density and thermal expansion coefficient of working fluids with temperature.

The empirical correlations for viscosity and the thermal conductivity of ferrofluid samples are obtained from the literature (Bahiraei & Hangi, 2016) and given in Eq. 2.13 and 2.14, respectively.

$$\mu_{nf} = 1.5474\, x\, 10^{10}(100\sigma + 1)^{0.358}T^{-5.3792} \tag{2.13}$$

$$k_{nf} = 0.05099(100\sigma + 1)^{0.07085}T^{0.4353} \tag{2.14}$$

Figure 2.6 shows the change in the viscosity and the thermal conductivity with concentration and temperature. The viscosity value and the difference between the concentrations reduce with the increasing temperature. With the increasing of concentrations and the temperature result in higher thermal conductivity values.

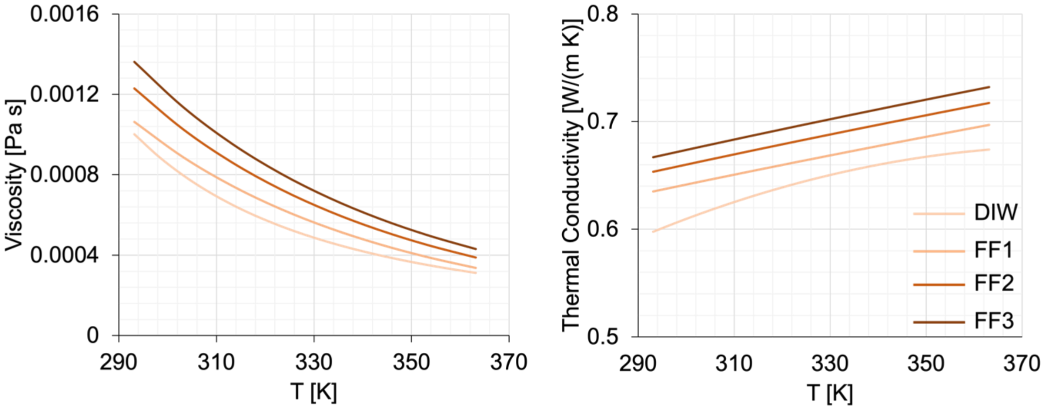

Figure 2.6 The change of viscosity and thermal conductivity of working fluids with temperature.

2.3 Performance Parameters

The driving mechanism of the SPNCLs is density gradient due to the temperature difference between the heater and cooler part, therefore T_{max} (T_5) and ΔT_{heater} (T_5-T_2) parameters can be used to compare characteristics of SPNCL at different operational cases (Çobanoğlu et al., 2019). Another parameter is effectiveness (ε), which is originally defined for heat exchangers, is a ratio of the actual heat transfer to the maximum possible heat transfer as given in Eq. 2.15 (Turgut & Doganay, 2014).

$$\varepsilon = \frac{T_5 - T_2}{T_5 - T_c}, \tag{2.15}$$

SPNCL's performance of heat transfer is evaluated by Nusselt number (Nu) as a dimensionless performance indicator.

$$Nu = \frac{UD}{k}, \tag{2.16}$$

In Eq. 2.16, U was evaluated by LMTD and it refers to the cooler's internal area (Misale et al., 2012). At the cooler, U was calculated by using the following equations:

$$U = \frac{Q}{\pi \, D \, L_c \, \Delta T_{LMTD}}, \tag{2.17}$$

$$\Delta T_{LMTD} = \frac{\Delta T_1 - \Delta T_2}{ln(\Delta T_1 / \Delta T_2 \,)}, \tag{2.18}$$

$$\Delta T_1 = T_6 - T_c, \tag{2.19}$$

$$\Delta T_2 = T_7 - T_c, \tag{2.20}$$

For understanding the buoyancy-driven heat transfer, Rayleigh number (Ra) is also investigated as a dimensionless performance indicator.

$$Ra = Gr_m Pr \tag{2.21}$$

Pr is Prandtl number and defined as (Cengel & Ghajar, 2011):

$$Pr \; = {}^{\mu c_p}/_{k}, \tag{2.22}$$

Gr_m, is the gravitational forces to shear stresses' ratio, is used for the assessment of the working fluid's natural convection intensity. For an SPNCL with a stable flow and constant heat flux boundary condition at the heater-end, Gr_m can be defined by:

$$Gr_m = \frac{D^3 \rho^2 Q_h H}{A \mu^3 c_p} \beta g \tag{2.23}$$

The system has also mixed convection characteristics since the momentum created on the heater-end results in an initial velocity in the fluid flow through cooler-end vice versa. This can be explained by natural circulation. For turbulent flow and laminar flow Re_{ss} can be predicted as a function of Gr_m :

$$Re_{ss} = B\left(\frac{Gr_m}{N_G}\right)^C, \tag{2.24}$$

B and C depend to geometrical parameters of the loop and thermophysical properties of fluid. For fully developed laminar flow, B = 0.1768 and C = 0.5 were defined by Vijayan (Vijayan, 2002). Here, $\mathrm{N_G}$ is effective loss coefficient and can be calculated as:

$$N_G = \frac{L_{total}}{D}\frac{\xi}{f}, \tag{2.25}$$

ξ can be described as local friction loss and taken from (Çengel & Cimbala, 2006) and f is the friction factor.

CHAPTER THREE
RESULTS AND DISCUSSIONS

3.1 Validation of the Numerical Model

3.1.1 Validation of the Horizontal Pipe

In SPNCLs, the working fluid in the system is stationary and isothermal everywhere at the beginning (Bozkir et al., 2021; Kumar et al., 2011). Switching on the heater power develops a temperature distribution along the heated wall as the heat diffuses towards the center of the tube as the time progresses, and this is almost pure conduction. When the thermal layers reach the center of the tube, convection currents are started to develop sideways on both sides of the heater-end and they are called as natural convection currents which are the major heat transfer mechanism from heated to unheated sections during the mass flow rate is zero or near zero. When the magnitude of the natural convection effects reaches the same order with the global velocity of the SPNCL (appreciable value of mass flow rate), the regime is called mixed convection. With the onset of the bulk fluid motion, the fluid begins to propagate either in clockwise or counter-clockwise direction throughout the SPNCL which is like forced convection through a pipe. At the transition from natural convection to mixed convection regime; the natural circulation currents, which provides bulk fluid motion, start to suppress natural convection currents and thus energy transfer by natural convection across the interface (Naveen et al., 2014). Since the natural circulation starts at the heater-end of the SPNCL, correct modeling of this section is crucial for accurate prediction of the SPNCL model.

The validation study for the heater-end of the SPNCmL was conducted for hydrodynamically developed and thermally developing pipe flow to understand natural convection effects and how the heat transfer is improved and thermal boundary layer is affected. A numerical model was developed and compared by using ANSYS CFX and COMSOL Multiphysics. Since pre-validated SPNCmL model was developed in ANSYS CFX (Cobanoglu & Karadeniz, 2020; Karadeniz et al., 2016), in this study results obtained by COMSOL Multiphysics were compared to ANSYS

CFX. To obtain hydrodynamically developed flow and eliminate back-flow at the outlet, tubes were added inlet and outlet of the heating section, respectively. The geometry and the boundary conditions of the system are presented in Figure 3.1.

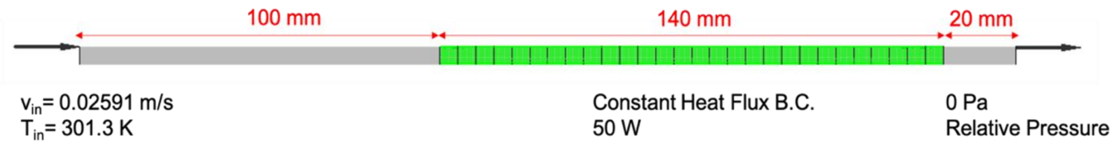

Figure 3.1 The geometry and the boundary conditions for validation of horizontal pipe.

Comparison of the change of local Nu along the heater-end with the well-known correlations of Shah, Shah & London (Shah, 1975; Shah & London, 1978), and Siegel (Siegel et al., 1958) proposed for hydrodynamically developed and thermally developing flow was compared. In the entrance region, the numerical results were in good agreement with correlations developed by Shah (Shah, 1975) as shown in Figure 3.2. However, Nu started to increase after this decreasing trend ($Gz^{-1} < 0.004$). Meyer and Everts (Meyer & Everts, 2018) explained the possible reason for this behavior by considering the natural convection effects. Higher Gr_m and lower Re result that the local Nu does not continue to decrease until flow becomes fully developed and then increase to reach a constant value under natural convection effects. Comparing to results of Shah, Shah & London (Shah, 1975; Shah & London, 1978) and Siegel (Siegel et al., 1958), Nu of COMSOL Multiphysics results increased by 96% and 71% at $Gz^{-1} = 0.028$, respectively (for ANSYS CFX Nu improved by 92% and 68% respectively.). Meyer and Everts (Meyer & Everts, 2018) also found that natural convection effects become significant with increasing heat flux and tube diameters, and it also decreases the thermal entry length and increases the Nu numbers for simultaneously developing flow in their experimental study. The Nu is higher up to 38% compared to results of Meyer and Everts (Meyer & Everts, 2018) at the condition of 4 mm pipe diameter and 8 kW/m^2 of constant heat flux in their study. Moreover, it is found that the thermal entrance length for forced convection laminar flow (Gz^{-1} = 0.05) is shortened for this study (Gz^{-1} = 0.004) due to the higher Gr_m and thus natural convection effects.

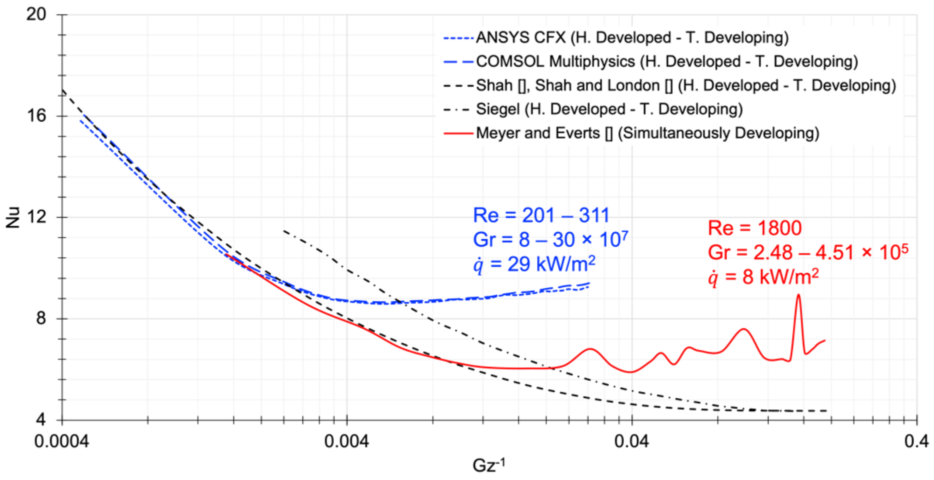

Figure 3.2 Validation of the hydrodynamically developed and thermally developing flow in horizontal pipe with Shah, Shah & London (Shah, 1975; Shah & London, 1978) and Siegel (Siegel et al., 1958) and simultaneously developing flow of Meyer & Everets (Meyer & Everts, 2018).

3.1.2 Validation of the SPNCmL

After evaluating the natural convection effects on horizontal pipe flow, validation study of the SPNCmL was conducted to evaluate the change of macro parameters accurately. For the SPNCmL case, the developed model by COMSOL Multiphysics was also validated with experimental results of Turgut and Doganay (Turgut & Doganay, 2014) and validation results were compared with numerical study of Çobanoğlu and Karadeniz (Cobanoglu & Karadeniz, 2020) considering normalized ε_N $(= \varepsilon_{numerical}/\varepsilon_{experimental})$, $T_{max,N}$ $(= T_{max,numerical}/T_{max,experimental})$ and $\Delta T_{heater,N}$ $(= \Delta T_{heater,numerical}/\Delta T_{heater,experimental})$ data as shown in Figure 3.3. Water-based Al_2O_3 nanofluids (1, 2 and 3 vol.%) were used as working fluids. Temperature as constant (293.15 K) and heat flux as constant (10, 30, and 50 W of heat rates for surface area of the heater surface area), boundary conditions were utilized to cooler and heater-ends, respectively. Further information on the system geometry and numerical model is given in (Cobanoglu & Karadeniz, 2020). It is clearly shown that ε_N can be predicted ± 20% error margin and T_{max} and ΔT_{heater} are generally overpredicted up to 16% and %20 compared to experimental data, respectively. The reason behind this overprediction can be explained by unmodelled heat storage of the pipe wall and insulation material.

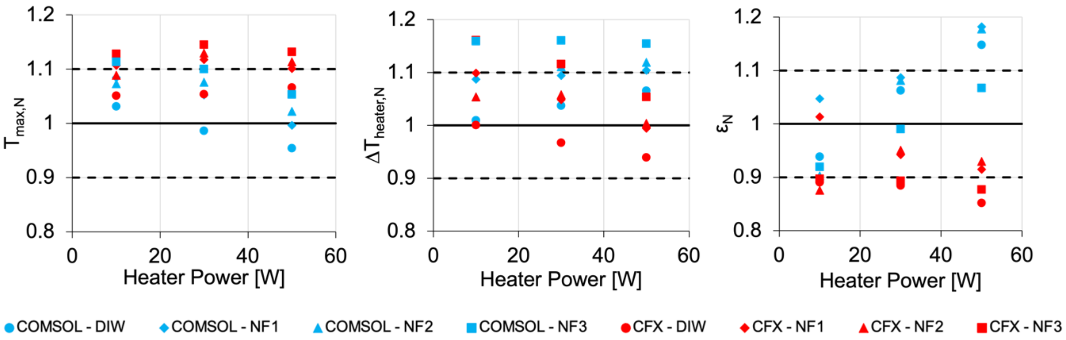

Figure 3.3 COMSOL Multiphysics model validation with experimental study of Turgut and Doganay (Turgut & Doganay, 2014) and numerical study of Çobanoğlu and Karadeniz (Cobanoglu & Karadeniz, 2020).

3.2 Performance of the Ferrofluid-based SPNCmL

The performance of the SPNCmL under magnetic field has been evaluated by the performance parameters of T_{max}, ΔT_{heater}, and ε. Figure 3.4 indicates a legend representation, and it can be used as source for all presented results on the performance of the ferrofluid-based SPNCmL in the rest of this work. The absence and presence of the magnetic field is defined as NoMF and MF, respectively. It is seen from Figures 3.5a and 3.5b that increasing the particle concentration and heater power result in higher temperatures in SPNCmL both in the MF and NoMF cases. Moreover, it is observed that the addition of magnetic field causes higher ΔT_{heater} and effectiveness (Figures 3.5b and 3.5c), and smaller T_{max} (Figure 3.5a) when compared with no magnetic field cases. Since the magnetization of fluid increases with the decrease of temperature (Phor & Kumar, 2019), the permanent magnet is located at the outlet of the cooler-end. Since the system is isolated, it means that the temperature at the heating inlet is also reduced. Therefore, it results in higher temperature difference through the hot side of the SPNCmL and thus heat transfer (increase in effectiveness up to 25%).

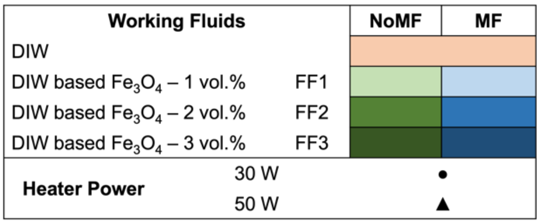

Working Fluids		NoMF	MF
DIW		🟧	🟧
DIW based Fe_3O_4 – 1 vol.%	FF1	🟩	🟦
DIW based Fe_3O_4 – 2 vol.%	FF2	🟩	🟦
DIW based Fe_3O_4 – 3 vol.%	FF3	🟩	🟦
Heater Power	30 W	●	
	50 W	▲	

Figure 3.4 A legend system showing colors of working fluids and symbols for different heater powers.

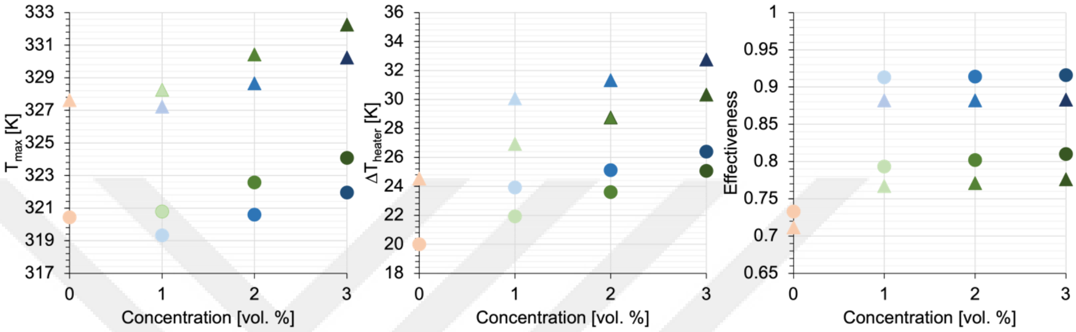

(a) (b) (c)

Figure 3.5 Effect of magnetic field on (a) T_{max}, (b) ΔT_{heater} and (c) ε.

To investigate the temperature and velocity distributions in the presence of magnetic field, we considered non-dimensional temperature and velocity (Eq. 3.1 and 3.2).

$$T^* = \frac{T_s}{T_{\max}} \tag{3.1}$$

$$V^* = \frac{V_s}{V_{max}} \tag{3.2}$$

Here, T_s and V_s are the local temperature [K] and velocity [m/s] values at the corresponding cross-sections. Figures 3.6 and 3.7 demonstrate the distribution of T^* and V^* at the inlet and outlet of the cooler and elbow inlet. T* distributions show that employing the magnetic field decreases the T_s values and it is obtained more yellowish and greenish colors at the center of the cooler inlet for 30 W and 50 W, respectively, and thus higher temperature difference between T_s and T_{max}. However, smaller temperature differences have been obtained for NoMF cases of ferrofluid-based SPNCmL, it can be seen from the orangish and yellowish distribution at the cooler inlet for 30W and 50 W, respectively. Similarly, higher temperature differences can be seen at the cross-sections of the cooler outlet and elbow inlet for both heater powers. Additionally, as the heater power increases the temperature distribution gets darker blue which means a higher temperature difference between T_s and T_{max} for all cases. However, the concentration of the ferrofluid has no significant effect on the T* distribution.

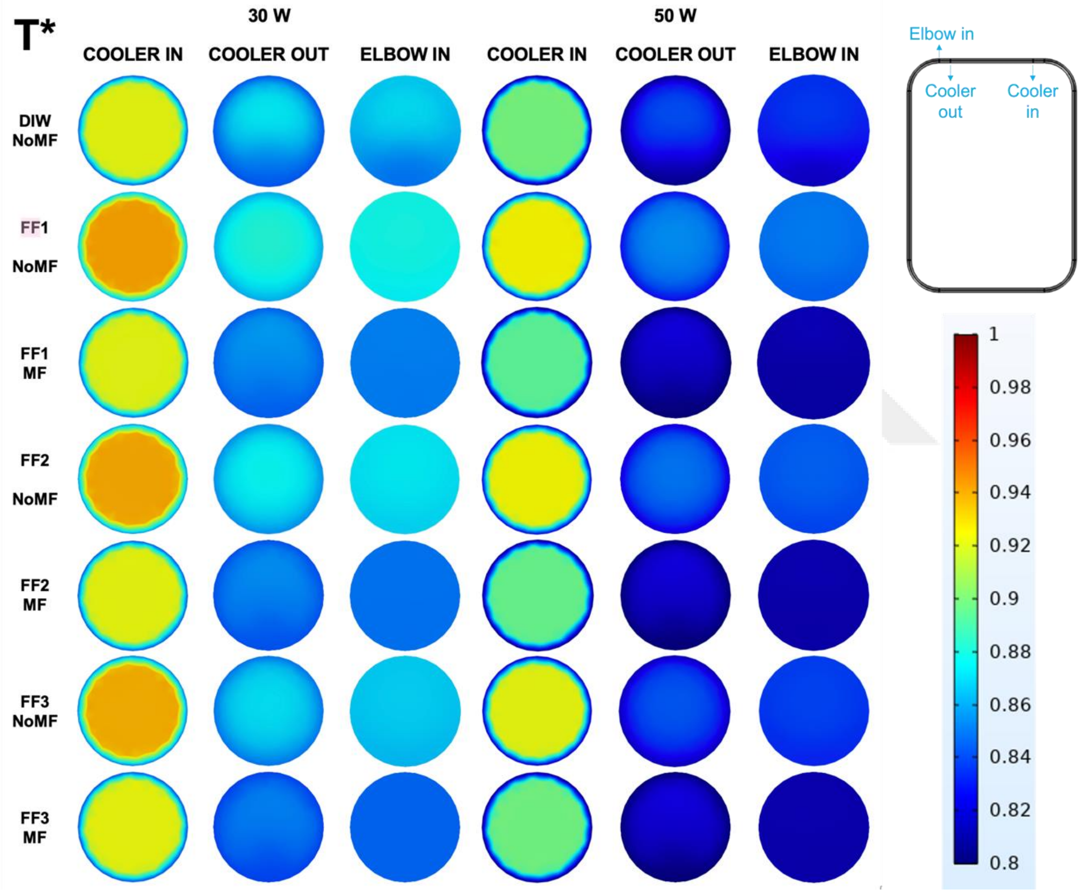

Figure 3.6 T* distribution at the critical cross-sections of cooling section.

The effect of the magnetic field is more clear for the V* distributions (Figure 3.7). Although there is no significant change in the V* in NoMF cases with the concentration increment, magnetic field’s utilization affects the V* distributions. In the presence of magnetic field, higher concentrations increase the intensity of the reddish area at the lower part of the cross-section for the cooler outlet which means higher V* values. In addition to magnetic field and concentration, higher V* values are obtained at higher heater powers at the cooler outlet. For the cross-sections at the elbow inlet, a tiny increment of V* values is obtained with the increase of concentration in SPNCmL working with 30 W of heater power under magnetic field. Unlike 30 W of heater power, V* values decrease with the increase of concentration at SPNCmL working with 50 W of heater power under magnetic field. The manipulation of the fluid flow by the magnetic field can be seen clearly from Figure 3.8 considering axial V* distributions. Moreover, the fluid direction is changeable in NoMF cases but employing MF results in counter-clockwise flow direction. Since the permanent magnet is placed below the pipe at the cooler outlet, a magnetic force due to the magnetic field gradient is higher at the lower part of the pipe. Hence, ferrofluid tends to move through the lower part of the pipe.

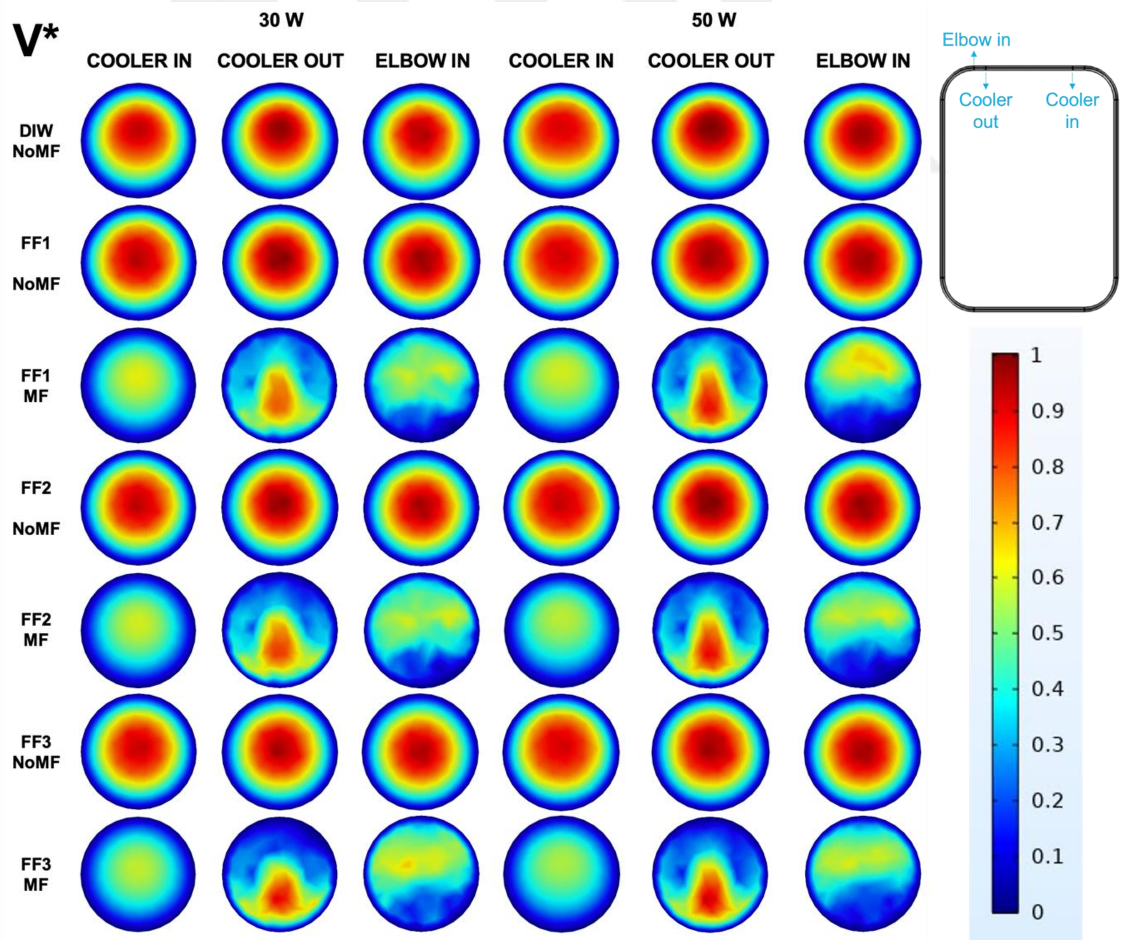

Figure 3.7 V* distribution at the critical cross-sections of cooling section

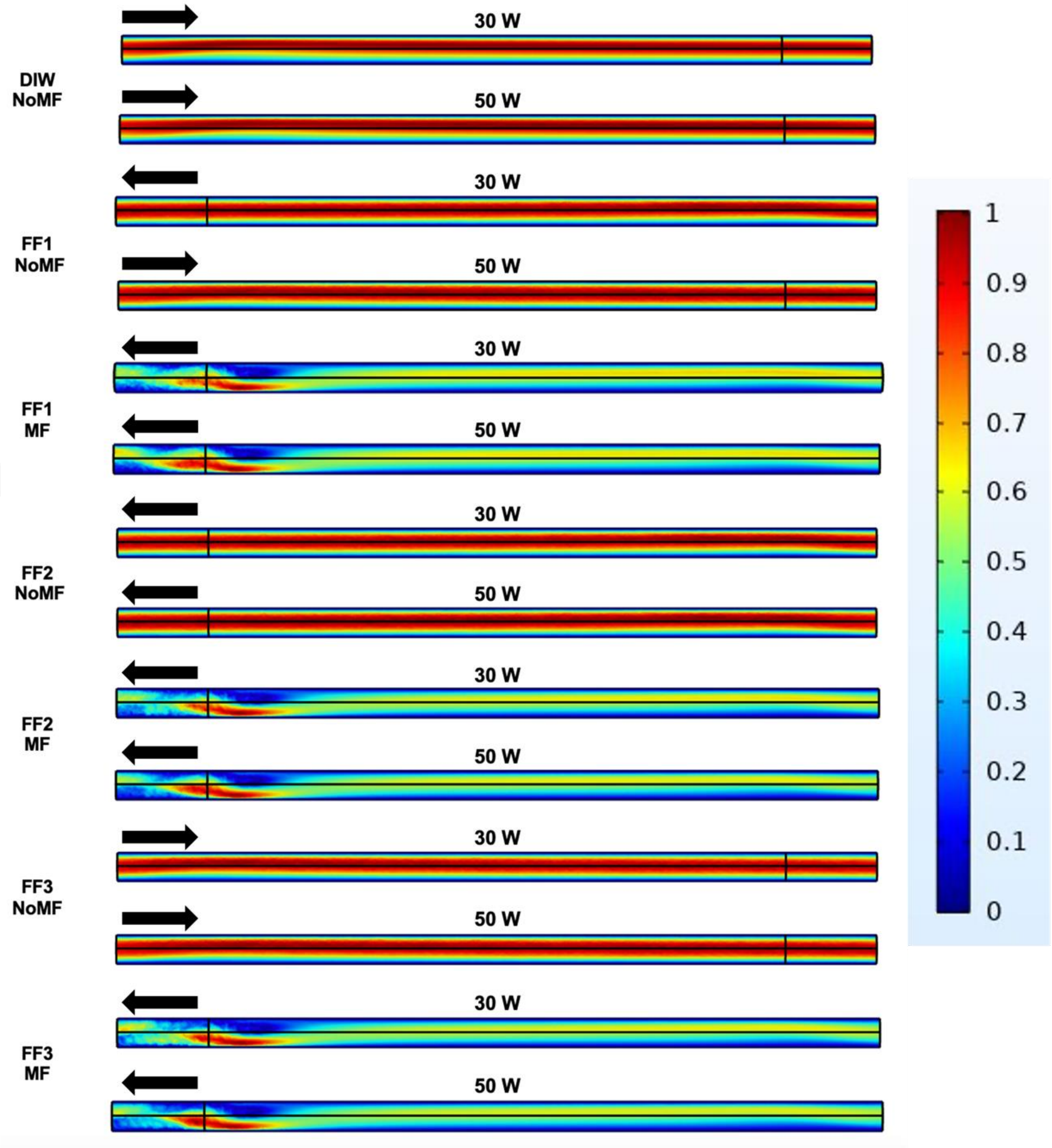

Figure 3.8 Axial V* distribution at the cooling section.

Figure 3.9 presents the change of Nu number with respect to Pr Re. Nu increases with the heater power for all working fluids at both MF and NoMF cases. For NoMF case, a tiny increment in the Nu is obtained for the FF1 case at both heater powers compared to the DIW, but it decreases with the increasing of concentration (FF2 and FF3). However, employing magnetic field results in a drastic enhancement of the Nu for all cases, but the increase of concentration still causes a reduction in the Nu. As aforementioned, locating the magnet at the cooler outlet improves the magnetization depending on the temperature gradient by reducing the temperature at the cooler outlet (Eq. 2.5). Reduction of the temperature at the cooler outlet results in higher temperature difference and thus higher Nu numbers compared to NoMF case.

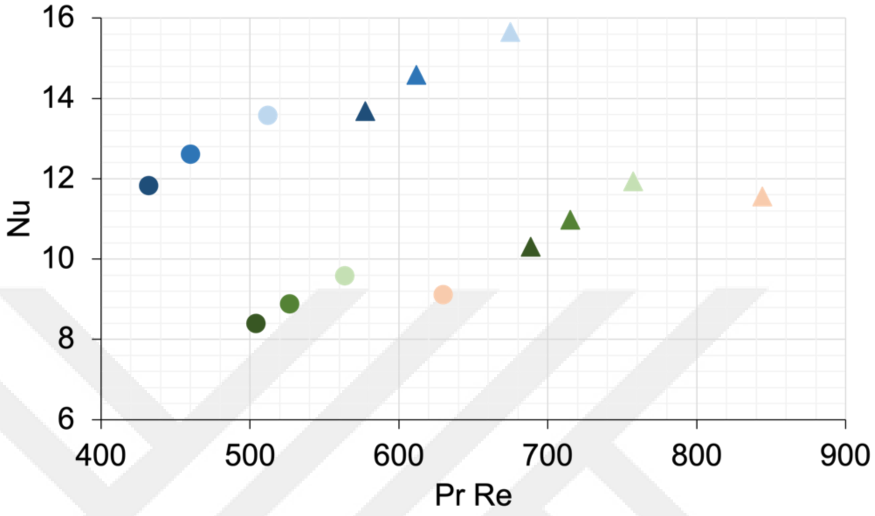

Figure 3.9 Change of Nu with Pr Re.

Since the magnetic field manipulates the fluid flow, it also affects the natural convection intensity in the SPNCmLs. Natural convection dominancy over forced convection is determined by the ratio of Gr_m/Re_{ss}^2. If the Gr_m/Re_{ss}^2 >>1 the natural convection prevails. Figure 3.10 shows that natural convection intensity increases with the heater power. Increase of concentration results in a slight reduction in the Gr_m/Re_{ss}^2 values for NoMF cases for both heater powers and case of 30 W under magnetic field. However, Gr_m/Re_{ss}^2value is constant for 50 W of heater power under magnetic field. Employing magnetic field affects temperature and velocity distributions on the fluid flow (Figure 3.6-3.8) which results in higher Gr_m/Re^2 values and thus higher Nu.

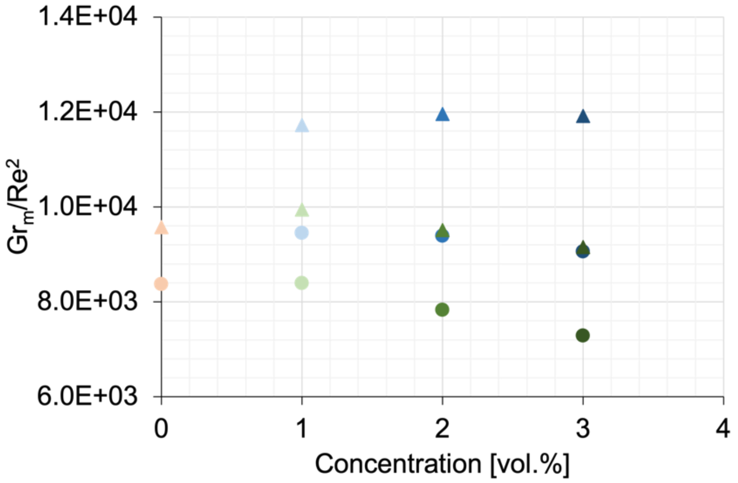

Figure 3.10 Effect of magnetic field on the natural convection dominancy considering Gr_m/Re^2.

CHAPTER FOUR
CONCLUSIONS

In this numerical study, it is aimed to investigate the magnetic field effects on the SPNCmL performance and the natural convection dominancy considering the fluid flow and the temperature distributions. The numerical model is developed in COMSOL Multiphysics by coupling magnetic field (no currents), heat transfer in fluids and fluid flow (laminar flow). Effect of the DIW-based Fe_3O_4 ferrofluids' (1-3 vol%.) concentration on SPNCmL performance is investigated under the conditions of different heater powers (30 and 50 W) and with/without magnetic field. Some key results are presented below:

- The validation study of the numerical model developed in COMSOL Multiphysics is conducted for heater-end of the SPNCmL under hydrodynamically developed and thermally developing pipe flow conditions and experimental SPNCmL study of the Turgut and Doganay (Turgut & Doganay, 2014). The results are compared with the data obtained by ANSYS CFX. Change of the Nu numbers in the horizontal pipe flow shows the dominancy of the natural convection effects all along the flow axis.

- The numerical model developed by COMSOL Multiphysics predicts the ε in the ± 20% error margin and T_{max} and ΔT_{heater} are generally overpredicted up to 16% and %20 compared to experimental data, respectively.

- Employing magnetic field to the ferrofluid-based SPNCmL causes higher ΔT_{heater} and ε, and smaller T_{max}.

- As seen from Figure 2.1, when the heater power and volumetric concentration are decreased, magnetic volume forces increase. Because, magnetization increases when the temperature decreases.

- The effect of the magnetic field has been shown by using T* and V* distributions at critical cross-sections of the cooler part. Higher temperature differences are obtained under the magnetic field. However, the concentration of the ferrofluid has no significant effect on the T* distribution.

- Under magnetic field, higher concentrations and higher heater powers increase the V* values at the cooler outlet for higher concentrations. However, the concentration effect is not significant for NoMF case.

- Locating the permanent magnet at the outlet of the cooler-end to strengthen magnetization of the working fluid, the temperature at the heating inlet is decreased. Therefore, it results in higher temperature difference and thus heat transfer (higher Nu numbers). However, the increase in concentration causes a reduction in the Nu.

- Considering the natural convection intensity under the magnetic field, Gr_m/Re^2 values are evaluated. For all cases Gr_m/Re_{ss}^2 >>1 which means that the natural convection is dominant. Gr_m/Re_{ss}^2 is constant for 50 W of heater power under magnetic field however there is a slight reduction is obtained for other cases.

REFERENCES

Alsangur, R., Doganay, S., Turgut, A., & Cetin, L. (2021). Magnetization behaviour of Fe3O4-water and gamma-Fe2O3-water magnetic nanofluids. *High Temperatures-High Pressures*, *50*(6), 385-394.

Andersson, H. I., & Valnes, O. A. (1998). Flow of a heated ferrofluid over a stretching sheet in the presence of a magnetic dipole. *Acta Mechanica*, *128*(1-2), 39-47.

Aursand, E., Gjennestad, M. A., Lervag, K. Y., & Lund, H. (2016). Potential of enhancing a natural convection loop with a thermomagnetically pumped ferrofluid. *Journal of Magnetism and Magnetic Materials*, *417*, 148-159.

Bahiraei, M., & Hangi, M. (2016). An empirical study to develop temperature-dependent models for thermal conductivity and viscosity of water-Fe3O4 magnetic nanofluid. *Materials Chemistry and Physics*, *181*, 333-343.

Bouhrour, A., & Kalache, D. (2017). Thermomagnetic convection of a magnetic nanofluid influenced by a magnetic field. *Thermal Science*, *21*(3), 1261-1274.

Bourantas, G. C., Skouras, E. D., Loukopoulos, V. C., & Burganos, V. N. (2014). Heat transfer and natural convection of nanofluids in porous media [Article]. *European Journal of Mechanics B-Fluids*, *43*, 45-56.

Bozkir, S., Çobanoğlu, N., Doganay, S., Karadeniz, Z., & Turgut, A. (2021). The Numerical Investigation on Natural Convection Effects in Single-Phase Natural Circulation Mini Loops. *The 3rd European Symposium on Nanofluids (ESNf), Iasi, Romania, Sep. 2021.*

Buschmann, M. H. (2020). Critical review of heat transfer experiments in ferrohydrodynamic pipe flow utilising ferronanofluids. *International Journal of Thermal Sciences*, *157*, 10.

Cengel, Y. A., & Ghajar, A. J. (2011). Heat and mass transfer (a practical approach, SI version). *McGraw-670 Hill Education, 671*, 52.

Chaudhary, V., Wang, Z., Ray, A., Sridhar, I., & Ramanujan, R. V. (2017). Self pumping magnetic cooling [Article]. *Journal of Physics D-Applied Physics, 50*(3), 8.

Choi, S. U. S., & Eastman, J. (1995). Enhancing thermal conductivity of fluids with nanoparticles. ASME-Publ.-Fed, vol. 231, pp. 99–106.

Cobanoglu, N., & Karadeniz, Z. H. (2020). Effect of Nanofluid Thermophysical Properties on the Performance Prediction of Single-Phase Natural Circulation Loops. *Energies, 13*(10), 23.

Çengel, Y. A., & Cimbala, J. M. (2006). *Fluid Mechanics: Fundamentals and Applications*. McGraw-HillHigher Education.

Çobanoğlu, N., Karadeniz, Z. H., & Turgut, A. (2019). Nanofluid-Based Single-Phase Natural Circulation Loops. In K. R. V. Subramanian, T. N. Rao, & A. Balakrishnan (Eds.), (pp. 59-76). CRC Press.

Doganay, S., Alsangur, R., & Turgut, A. (2019). Effect of external magnetic field on thermal conductivity and viscosity of magnetic nanofluids: a review. *Materials Research Express*, *6*(11).

Doganay, S., & Turgut, A. (2015). Enhanced effectiveness of nanofluid based natural circulation mini loop. *Applied Thermal Engineering*, *75*, 669-676.

Fruh, W.-G. (2005). Heat transfer enhancement by thermomagnetic convection. *Sustainable (Bio)Chemical Process Technology incorporating on Process*

Intensification 6. Proceedings of 6th International Process Intensification Conference, Delft, 27-29 September 2005. BHR Group LTd., pp. 47- 56.

Garibaldi, P., & Misale, M. (2008). Experiments in single-phase natural circulation miniloops with different working fluids and geometries. *Journal of Heat Transfer-Transactions of the Asme*, *130*(10), 5.

Gijs, M. A. M., Lacharme, F., & Lehmann, U. (2010). Microfluidic Applications of Magnetic Particles for Biological Analysis and Catalysis. *Chemical Reviews*, *110*(3), 1518-1563.

Grosu, Y., Faik, A., Ortega-Fernandez, I., & D'Aguanno, B. (2017). Natural Magnetite for thermal energy storage: Excellent thermophysical properties, reversible latent heat transition and controlled thermal conductivity. *Solar Energy Materials and Solar Cells*, *161*, 170-176.

Ho, C. J., Chung, Y. N., & Lai, C. M. (2014). Thermal performance of Al2O3/water nanofluid in a natural circulation loop with a mini-channel heat sink and heat source. *Energy Conversion and Management, 87*, 848-858.

Holcomb, G. R. (2019). A review of the thermal expansion of magnetite. *Materials at High Temperatures*, *36*(3), 232-239.

Karadeniz, Z., Doganay, S., & Turgut, A. (2014). Numerical study on nanofluid based single phase natural circulation mini loops. *Proceedings of CONV-14: International Symposium on Convective Heat and Mass Transfer. June 8 - 13, 2014, Kusadasi, Turkey.*

Karadeniz, Z. H., Doganay, S., & Turgut, A. (2016). Numerical study on nanofluid based single phase natural circulation mini loops: A steady 3D approach. *High Temperatures-High Pressures*, *45*(4), 321-335.

Karimi-Moghaddam, G., Gould, R. D., & Bhattacharya, S. (2014). A Nondimensional Analysis to Characterize Thermomagnetic Convection of a Temperature Sensitive Magnetic Fluid in a Flow Loop. *Journal of Heat Transfer-Transactions of the Asme, 136*(9), 7.

Karimi-Moghaddam, G., Gould, R. D., Bhattacharya, S., & Asme. (2013). Numerical investigation of electronic liquid cooling based on the thermomagnetic effect. *Proceedings of the Asme International Mechanical Engineering Congress and Exposition - 2012, Vol 7, Pts a-D*, 1441-1447.

Koca, H. D., Doganay, S., & Turgut, A. (2017). Thermal characteristics and performance of Ag-water nanofluid: Application to natural circulation loops. *Energy Conversion and Management, 135*, 9-20.

Kole, M., & Khandekar, S. (2021). Engineering applications of ferrofluids: A review. *Journal of Magnetism and Magnetic Materials, 537*, 168222.

Kumar, N., Doshi, J. B., & Vijayan, P. K. (2011). Investigations on the role of mixed convection and wall friction factor in single-phase natural circulation loop dynamics. *Annals of Nuclear Energy, 38*(10), 2247-2270.

Lian, W., Xuan, Y., & Li, Q. (2009). Characterization of miniature automatic energy transport devices based on the thermomagnetic effect. *Energy Conversion and Management, 50*(1), 35-42.

Lian, W. L., Xuan, Y. M., Li, Q., & Asme. (2010). Investigation on multi-pump liquid-cooling loop based on thermomagnetic effect. *Proceedings of the Asme International Heat Transfer Conference - 2010 , Vol 3: Combustion, Conduction, Electronic Cooling, Evaporation,Two-Phase Flow*, 417-423.

Love, L. J., Jansen, J. F., McKnight, T. E., Roh, Y., Phelps, T. J., Yeary, L. W., & Cunningham, G. T. (2005). Ferrofluid field induced flow for microfluidic applications. *Ieee-Asme Transactions on Mechatronics*, *10*(1), 68-76.

Matsuki, H., Yamasawa, K., & Murakami, K. (1977). Experimental considerations on a new automatic cooling device using temperature-sensitive magnetic fluid. *IEEE Transactions on Magnetics*, *13*(5), 1143-1145.

Meyer, J. P., & Everts, M. (2018). Single-phase mixed convection of developing and fully developed flow in smooth horizontal circular tubes in the laminar and transitional flow regimes. *International Journal of Heat and Mass Transfer*, *117*, 1251-1273.

Misale, M., Devia, F., & Garibaldi, R. (2012). Experiments with Al2O3 nanofluid in a single-phase natural circulation mini-loop: Preliminary results [Article]. *Applied Thermal Engineering*, *40*, 64-70.

Misale, M., Garibaldi, P., Passos, J. C., & de Bitencourt, G. G. (2007). Experiments in a single-phase natural circulation mini-loop. *Experimental Thermal and Fluid Science*, *31*(8), 1111-1120.

Mohan, M., Thomas, S., Taha-Tijerina, J., Narayanan, T. N., Sobhan, C. B., Ajayan, P. M., & Asme. (2014). Heat transfer studies in thermally conducting and electrically insulating nano-oils in a natural circulation loop. *Proceedings of the Asme International Mechanical Engineering Congress and Exposition, 2013, Vol 6b*, 7.

Naveen, K., Iyer, K. N., Doshi, J. B., & Vijayan, P. K. (2014). Investigations on single-phase natural circulation loop dynamics part 1: Model for simulating start-up from rest. *Progress in Nuclear Energy*, *76*, 148-159.

Nayak, A. K., Gartia, M. R., & Vijayan, P. K. (2008). An experimental investigation of single-phase natural circulation behavior in a rectangular loop with Al2O3 nanofluids. *Experimental Thermal and Fluid Science*, *33*(1), 184-189.

Nguyen, N. T. (2012). Micro-magnetofluidics: interactions between magnetism and fluid flow on the microscale. *Microfluidics and Nanofluidics*, *12*(1-4), 1-16.

Phor, L., & Kumar, V. (2019). Self-cooling device based on thermomagnetic effect of MnxZn1-xFe2O4 (x=0.3, 0.4, 0.5, 0.6, 0.7)/ferrofluid. *Journal of Materials Science-Materials in Electronics*, *30*(10), 9322-9333.

Sahu, M., Sarkar, J., & Chandra, L. (2021). Effects of various modeling assumptions on steady-state and transient performances of single-phase natural circulation loop. *International Communications in Heat and Mass Transfer*, *124*, 13.

Shah, R. K. (1975). Thermal entry length solutions for the circular tube and parallel plates. *Proceedings of 3rd national heat and mass transfer conference. In Proceedings of the 3rd National Heat and Mass Transfer Conference, Bombay, India, 11–13 December 1975; Indian Institute of Technology: Bombay, India, 1975; Volume I, pp.* 11–75.

Shah, R. K., & London, A. L. (1978). Laminar flow forced convection in ducts (Vol. 1). Elsevier. *New York: Academic Press.*

Sheikholeslami, M., & Ganji, D. D. (2014). Ferrohydrodynamic and magnetohydrodynamic effects on ferrofluid flow and convective heat transfer. *Energy*, *75*, 400-410.

Siegel, R., Sparrow, E. M., & Hallman, T. M. (1958). Steady laminar heat transfer in a circular tube with prescribed wall heat flux. *Applied Scientific Research, Section A*, *7*(5), 386-392.

T. M. Group, M. Retrieved October 20, 2020, from http://www.tenmet.co.uk/product-range/6/magnetite

Turgut, A., & Doganay, S. (2014). Thermal performance of a single phase natural circulation mini loop working with nanofluid. *High Temperatures-High Pressures*, *43*(4), 311-320.

Tzirtzilakis, E. E., & Xenos, M. A. (2013). Biomagnetic fluid flow in a driven cavity. *Meccanica*, *48*(1), 187-200.

Vijayan, P. K. (2002). Experimental observations on the general trends of the steady state and stability behaviour of single-phase natural circulation loops. *Nuclear Engineering and Design*, *215*(1-2), 139-152.

Xuan, Y. M., & Lian, W. L. (2011). Electronic cooling using an automatic energy transport device based on thermomagnetic effect [Article]. *Applied Thermal Engineering*, *31*(8-9), 1487-1494.

Yu, W. H., France, D. M., Routbort, J. L., & Choi, S. U. S. (2008). Review and comparison of nanofluid thermal conductivity and heat transfer enhancements. *Heat Transfer Engineering*, *29*(5), 432-460.

Zhou, S. Q., & Ni, R. (2008). Measurement of the specific heat capacity of water-based Al2O3 nanofluid [Article]. *Applied Physics Letters*, *92*(9), 3.

APPENDICES

APPENDIX-1: Nomenclature

SPNCmL	Single phase natural circulation mini loop
NdFeB	Neodymium magnet
T	Temperature [K]
ΔT_{heater}	Temperature differences [K]
ε	Effectiveness
T_{max}	Maximum temperature [K]
DIW	De-ionized water
SPNCL	Single phase natural circulation loop
Al_2O_3	Aluminium oxide
Ag	Silver
Mn	Manganez
AETD	Automatic energy transport device
Fe_3O_4	Magnetite
μ_0	Free space permeability [H/m]
μ_r	Relative permeability [H/m]
B_r	Remanence of the permanent magnet [T]
H	Magnetic field intensity [A/m]
V_m	Magnetic scalar potential [A]
F_m	Magnetic Force [N/m^3]
Q_m	Magnetocaloric effect [W/m^3]
U	Velocity through x-direction [m/s]

v	Velocity through y-direction [m/s]
w	Velocity through z-direction [m/s]
M	Magnetization [A/m]
K	Pyromagnetic coefficient [A/(m*K)]
T_{curie}	Curie temperature [K]
F_{ext}	External forces [N/m^3]
Q_p	Pressure work [W/m^3]
ρ	Density [kg/m^3]
μ	Viscosity [Pa*s]
C_p	Specific heat [J/(kg*K)]
$\mathbf{F_b}$	Bouyancy force [N/m^3]
k	Thermal conductivity [W/(m*K)]
β	Thermal expansion coefficient [1/K]
Nu	Nusselt Number
U	Overall heat transfer coefficient [W/(m^2*K)]
LMTD	Logarithmic mean temperature difference [K]
Ra	Rayleigh number
Pr	Prandtl number
Gr	Grashof number
Re	Reynold number
N_G	Effective loss coefficient
ξ	Local friction loss
f	Friction factor
L_{total}	Total length [m]

D	Diameter [m]
Gz	Graetz number
NoMF	No magnetic field
MF	Magnetic field
FF	Ferrofluid
NF	Nanofluid
T_s	Local temperature [K]
V_s	Local velocity [m/s]